

# Functional Analysis of *HSF4* Mutations Found in Patients With Autosomal Recessive Congenital Cataracts

Kate Merath, Adam Ronchetti, and Duska J. Sidjanin

Department of Cell Biology, Neurobiology, and Anatomy, Medical College of Wisconsin, Milwaukee, Wisconsin

Correspondence: Duska J. Sidjanin, Department of Cell Biology, Neurobiology, and Anatomy, Human and Molecular Genetics Center, Medical College of Wisconsin, Milwaukee, WI 53226; dsidjani@mcw.edu.

KM and AR contributed equally to the work presented here and should therefore be regarded as equivalent authors.

Submitted: April 23, 2013

Accepted: August 31, 2013

Citation: Merath K, Ronchetti A, Sidjanin DJ. Functional analysis of *HSF4* mutations found in patients with autosomal recessive congenital cataracts. *Invest Ophthalmol Vis Sci*. 2013;54:6646-6654. DOI:10.1167/iov.13-12283

**PURPOSE.** The goal of this study was to functionally evaluate three previously uncharacterized heat shock factor protein 4 (*HSF4*) mutations (c.595\_599delGGGCC, c.1213C>T, c.1327+4A>G) encoding mutant *HSF4* proteins (G199EfsX15, R405X, and M419GfsX29) with missing C-terminal ends. These *HSF4* mutations were previously identified in families with congenital autosomal recessive cataracts.

**METHODS.** FLAG-tagged recombinant wild type (WT) and mutant *HSF4* proteins were analyzed using the protein stability assay, cellular immunofluorescence, Western blotting, electrophoretic mobility shift assay (EMSA), and reporter activation.

**RESULTS.** *HSF4* mutant proteins did not differ in the protein turnover rate when compared with WT *HSF4*. Immunofluorescence revealed that WT and mutant *HSF4* proteins were properly trafficked to the nucleus. EMSA analysis revealed that the G199EfsX15 and M419GfsX29 proteins exhibited decreased heat shock element (HSE)-mediated DNA binding, whereas the R405X mutant exhibited increased HSE-mediated DNA binding when compared with WT *HSF4*. All three *HSF4* mutant proteins exhibited abolished HSE-mediated luciferase reporter activation. Detailed evaluation of the C-terminal region identified three novel domains: two activation domains and one repression domain.

**CONCLUSIONS.** The three *HSF4* autosomal recessive mutations evaluated here result in a loss of *HSF4* function due to a loss of regulatory domains present at the C-terminal end. These findings collectively indicate that the transcriptional activation of *HSF4* is mediated by interactions between activator and repressor domains within the C-terminal end.

Keywords: congenital, cataracts, *HSF4*, mutation

Mutations in the heat shock transcription factor 4 (*HSF4*) lead to autosomal dominant (AD) and autosomal recessive (AR) forms of congenital cataracts.<sup>1-5</sup> *HSF4* belongs to the heat shock family of transcription factors (HSFs) characterized by the evolutionarily highly conserved winged helix-turn-helix DNA binding motif. The role of HSFs is in the transactivation of downstream target genes, via binding to the heat shock element consensus sequence (5'nGAAn-3'), in response to environmental and developmental stresses.<sup>6,7</sup> *HSF4* binds DNA as a homotrimer and trimerization of *HSF4* subunits is mediated by the hydrophobic repeat region (HR-A/B).<sup>8</sup> Unlike other members of the HSF family, *HSF4* lacks the carboxyl-terminal heptad repeat (HR-C) region that is responsible for the monomerization of HSF subunits, and as such, *HSF4* has been shown to be constitutively multimeric.<sup>9</sup> Two alternatively spliced transcript variants, *HSF4a* and *HSF4b*, have been identified,<sup>10</sup> but only the *HSF4b* variant was identified as being expressed in the lens.<sup>5,11</sup> Therefore, mutations in *HSF4* identified in families with congenital cataracts are due to altered function of the *HSF4b* protein.

To date, nine different mutations have been identified in the *HSF4* gene (Table). Five *HSF4* mutations (A19D, R73H, I86V, L114P, R119C) reside within the highly conserved helix-turn-helix DNA binding domain and functional analysis of these five mutations revealed that these mutant proteins exhibit compromised HSE-mediated DNA binding.<sup>12</sup> Functional analysis of an additional *HSF4* mutation (R175P) residing within the *HSF4*

trimerization domain revealed compromised trimerization and consequently compromised HSE-mediated DNA binding.<sup>12</sup> The functional analysis of *HSF4* missense mutations has highlighted the necessity of DNA binding and trimerization domains for the normal functionality of *HSF4*. However, three additional *HSF4* mutations were identified in families with autosomal recessive congenital cataracts.<sup>3-5</sup> Specifically, a 5 base pair (bp) deletion (*HSF4* c.595\_599delGGGCC) was identified in a small consanguineous family where affected family members presented cataracts at birth without any other ocular or systemic abnormalities.<sup>3</sup> The *HSF4* c.1213C>T mutation was identified in a large consanguineous family, where affected family members presented cataracts at birth or early on in infancy without any additional ocular or systemic abnormalities.<sup>4</sup> Finally, the *HSF4* c.1327+4A>G mutation was identified in a large consanguineous family, where affected members similarly exhibited total cataracts present at birth associated with nystagmus, although no other ocular or systematic abnormalities were identified.<sup>5</sup> These three uncharacterized *HSF4* mutations are predicted to encode putative truncated *HSF4* proteins with missing C-terminal ends. The mechanism underlying the way in which a loss of the C-terminal domain affects *HSF4* function has never been investigated.

As a part of this study, we undertook the functional evaluation of three autosomal recessive *HSF4* (c.595\_599delGGGCC, c.1213C>T, c.1327+4A>G) mutations. Our results revealed that the truncated *HSF4* mutant proteins are loss-of-function muta-

TABLE. *HSF4* Mutations Identified in Families With AD and AR Congenital Cataracts

<i>HSF4</i> Genotype	<i>HSF4</i> Protein	Mode of Inheritance	Cataract Phenotype	Reference
c.56C>A	p. A19D	De novo	Not described	Bu et al. <sup>1</sup>
c.218G>A	p. R73H	AD	Total white	Ke et al. <sup>2</sup>
c.256A>G	p. I86V	Sporadic	Not described	Bu et al. <sup>1</sup>
c.341T>C	p. L114P	AD	Lamellar with a transparent nucleus	Bu et al. <sup>1</sup>
c.355C>T	p. R119C	AD	Zonular stellate with an anterior polar opacity	Bu et al. <sup>1</sup>
c.524G>C	p. R175P	AR	Not described	Forsheve et al. <sup>3</sup>
c.595_599delGGGC	p. G199EfsX15	AR	Not described	Forsheve et al. <sup>3</sup>
c.1213C>T	p. R405X	AR	Not described	Sajjad et al. <sup>4</sup>
c.1327+4A>G	p. M419GfsX29	AR	Total	Smaoui et al. <sup>5</sup>

tions due to the loss of novel regulatory domains identified within the *HSF4* C-terminal end essential for the proper *HSF4* function.

## MATERIALS AND METHODS

### *HSF4* cDNA Constructs

The WT human *HSF4b* cDNA in pCMV6-XL4 vector was purchased from OriGene Technologies, Inc. (Rockville, MD). Following digestion with *EcoRI* and *SmaI*, *HSF4* cDNA was cloned into the pFLAG-CMV-5 vector (Sigma-Aldrich, St. Louis, MO). To generate an in-frame WT *HSF4b* C-terminal FLAG tag, a 267-bp sequence containing the stop codon and the 3'UTR was removed using a mutagenesis kit (Phusion Site-Directed Mutagenesis Kit; Thermo Fisher Scientific/Finnzymes Oy, Vantaa, Finland) following manufacturer's protocol with primers (F) 5'-phos-GATTACAAGGACGACGATGACAAG-3' and (R) 5'-phos-GGGGGAGGGACTGGCTTCCG-3'. To generate the R405X mutant, we used a mutagenesis kit (QuikChange II Site-Directed Mutagenesis Kit; Stratagene, La Jolla, CA) following the manufacturer's protocol with the primers listed in Supplementary Table S1. To generate the G199EfsX15 and M419GfsX29 *HSF4* deletion mutants, as well as C-terminal deletion mutants  $\Delta$ 425-492,  $\Delta$ 435-492,  $\Delta$ 445-492,  $\Delta$ 455-492, and  $\Delta$ 246-319, the mutagenesis kit (QuikChange II Site-Directed Mutagenesis Kit; Thermo Fisher Scientific/Finnzymes Oy) was used following manufacturer's protocol with the primers in Supplementary Table S1. Plasmids were purified with a plasmid DNA kit (QIAGEN Plasmid Mini Kit; QIAGEN, Venlo, Limburg) and a plasmid DNA purification kit (PureLink HiPure Plasmid Midiprep Kit; Life Technologies Corp., Carlsbad, CA). All plasmid construct sequences were confirmed by direct sequencing.

### Cell Culture, Transfection, Nuclear Extracts, and Immunofluorescence

HEK293 cells, HeLa, and immortalized human lens epithelial (HLE-B3) cells were obtained from ATCC and were cultured using the supplier's cell-line specific protocols. All transfections were done using a transfection reagent (Lipofectamine LTX with Plus Reagent; Life Technologies Corp.) following the manufacturer's protocol for each cell line. Following transfection, nuclear and cytoplasmic extracts were collected from the transfected cells using an extraction kit (CellLytic NuCLEAR Extraction Kit; Sigma-Aldrich) and following the manufacturer's protocol as previously described.<sup>13</sup> For immunofluorescence, HeLa cells were transfected with plasmid DNA and then grown on coverslips in 12-well plates; 24 hours later, cells were

fixed in 4% paraformaldehyde for 1 hour at room temperature (RT), permeabilized with PBS + 0.25% Triton X-100 for 10 minutes, blocked with 1% BSA in 1× PBST for 30 minutes at RT and incubated for 1 hour at RT with 10  $\mu$ g/mL mouse monoclonal FLAG antibody (Sigma-Aldrich) in 1% BSA in 1× PBST followed by an incubation with 1:100 goat anti-mouse (DyLight 488; Abcam, Cambridge, England) in the dark. DNA was stained with 3 ng/mL DAPI (Sigma-Aldrich). The slides were mounted with mounting medium (VECTASHIELD; Vector Laboratories, Burlingame, CA). All slides were visualized with a fluoroscope (Nikon Eclipse 600; Nikon Corp., Tokyo, Japan).

### Protein Stability

HEK293 cells were seeded at  $1.6 \times 10^6$  cells/100 mm dish in complete media containing 10% fetal bovine serum-modified Eagle's medium (FBS-MEM) for 16 hours and then transfected with 14  $\mu$ g of either wild type or mutant clones. Following transfection, the medium was replaced with 12 mL fresh MEM + 10% FBS and incubated for an additional 24 hours at which time, the cells were divided into 24-well plates. Cells were incubated with cycloheximide (20 mg/mL) for 0 (DMSO vehicle only), 0.5, 1, 2, 4, and 6 hours; lysed; and subjected to Western blotting. Signals from Western blot analysis were analyzed with photo editing software (Adobe Photoshop; Adobe Systems, San Jose, CA) and plotted using data from three independent experiments.

### Western Blot Analysis

Nuclear extracts were electrophoresed on a 10% SDS-polyacrylamide gel, transferred to a polyvinylidene difluoride-plus transfer membrane (GE Water and Process Technologies Magna; GE Healthcare Life Sciences, Pittsburgh, PA) and immunoblotted using a FLAG monoclonal antibody at 1:1000 at 4°C O/N (Sigma-Aldrich), or a histone 3 antibody at 1:500 at RT for 1 hour (Cell Signaling, Danvers, MA). An HRP goat anti-mouse conjugated secondary antibody was used at 1:5000 (Jackson ImmunoResearch Laboratories Inc., West Grove, PA). The signal was detected with a commercial analysis system (ECL Western Blotting Analysis System; GE Healthcare Life Sciences).

### Electrophoretic Mobility Shift Assay

Oligonucleotide labeling, binding, and electrophoresis were done using an assay system (Gel Shift Assay System; Promega Corp., Madison, WI) following the manufacturer's protocol. The oligonucleotide 5'-TGACATCACCATTCCAAGCTTCA-CAAGA-3' containing the HSE motif (underlined) was used for the binding assay. For oligonucleotide labeling, ATP [ $\gamma$ -<sup>32</sup>P]-

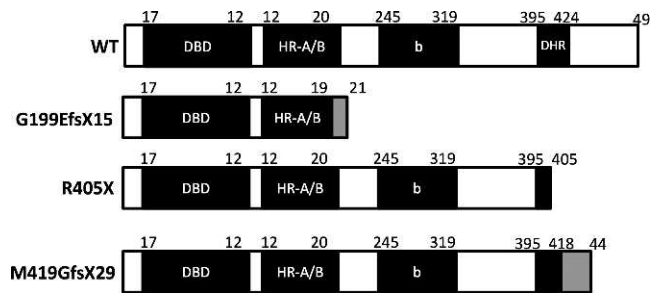


**FIGURE 1.** Localization of the functional domains in WT and mutant *HSF4* proteins. WT schematic represents *HSF4b* (NP\_001035757), whereas G199EfsX15, R405X, and M419GfsX29 are predicted proteins encoded by previously identified *HSF4* mutations c.595\_599delGGGCC, c.1213C>T, and c.1327+4A>G, respectively. Depicted as *black boxes* are: DNA binding domain (DBD), oligomerization domain (HR-A/B), and *HSF4b*-specific sequence (b) that differs between *HSF4a* and *HSF4b* and DHR region previously identified.<sup>10</sup> *Gray boxes* depict additions of the novel 14 aa (EQCRRQEKAVPDAG) in G199EfsX15 and 28 aa (GRTPRSGPHSCWMSRRPWAEQPWACLGL) in M419GfsX29 mutant proteins resulting from frame-shifts. *Numbers on the top of each box* represent the amino acid residues.

3000 Ci/mmol 10 mCi/mL was used following manufacturer's protocol. To determine the specificity of the HSE-binding reactions were set up containing 1.75 pmol unlabeled HSE containing oligo as a specific competitor, 1.75 pmol SP1 consensus oligo as a nonspecific competitor, or 1  $\mu$ L mouse monoclonal Anti-FLAG antibody (Sigma-Aldrich) for a super-shift following the manufacturer's protocol. All binding reactions were incubated at RT for 20 minutes and electrophoresed at RT in 1 $\times$  TAE on a 4% acrylamide (40:1 acrylamide:bisacrylamide) gel for 1 hour at 250 V. Following electrophoresis, gels were transferred onto 3M paper, covered with plastic wrap, dried on a gel drier, and exposed to x-ray film at  $-70^{\circ}\text{C}$  for 30 minutes.

### Luciferase Assay

The pGL3-HSE-GC luciferase reporter was generated by PCR-amplifying a DNA fragment ( $-734$  to  $+3$ ) from the promoter of human  $\gamma$ C-crystallin (NM\_020989) containing distal and proximal HSE elements<sup>14</sup> using the following primers: (F) 5'-AGGCGGCCTGAGTCCAAAGCTCACTCTT-3' and 5'-CATGGCTGGTTGACACGGATGATGCGAGTT-3'. The pGL3-HSE-AB luciferase reporter was generated by PCR-amplifying a DNA fragment ( $-544$  to  $+1$ ) from the promoter of human  $\alpha$ B-crystallin (NM\_001885) containing the HSE element using the following primers (F) 5'-CAACAAGAGCTCCCAGTCAGACACC-TAGTTCTGCTCTC and (R) 5'-CGACTCTGCATTCATCTAGC-CACCTCGAGAACAAC and was subsequently cloned into the *SacI* and *XbaI* sites of pGL3Basic using standard protocols. Approximately  $1.25 \times 10^5$  HEK293 or HLE-B3 cells per well were seeded in 24-well dishes in complete media containing 10% FBS-MEM for 16 hours and then transfected with 300 ng/well of effector DNA, 110 ng/well reporter DNA, and 60 ng/well pcDNA<sub>lacZ</sub> (for normalization of transfection efficiency). Following transfection, media was replaced with 1 mL fresh 10% FBS-MEM and incubated for an additional 24 hours, after which cells were lysed using a Luciferase assay system (Promega Corp.).  $\beta$ -galactosidase activity was measured in lysates using a  $\beta$ -galactosidase assay system (Promega Corp.). Luciferase activity was subsequently normalized to  $\beta$ -galactosidase activity. All luciferase assays were performed a minimum of three times, each time in triplicate. Each data point represents a minimum of three separate experiments and each

data point is represented as mean  $\pm$  SEM. Significance was calculated via a *t*-test (GraphPad Prism; GraphPad Software, La Jolla, CA), where  $P < 0.05$  was considered significant.

## RESULTS

### HSF4 Autosomal Recessive Mutations Resulting in a Loss of C-Terminus

The *HSF4* c.595\_599delGGGCC deletion<sup>3</sup> was predicted to result in a putative G199EfsX15 protein exhibiting a frame-shift starting with the G199 residue, an addition of 14 novel amino acids (EQCRRQEKAVPDAG), and a premature stop codon (Fig. 1). The Basic Local Alignment Search Tool (BLAST) analysis of the 14 newly added residues (EQCRRQEKAVPDAG) did not reveal significant similarity to any known protein. The *HSF4* c.1213C > mutation<sup>4</sup> was predicted to result in an R405 to stop codon exchange and a loss of 87 amino acids from the C-terminal end (Fig. 1). Finally, the *HSF4* c.1327+4A>G mutation<sup>5</sup> identified at the +4 position of intron 12, resulted in aberrant *HSF4* splicing and skipping of exon 12, a frame shift following the M419 residue, an addition of 28 novel residues (GRTPRSGPHSCWMSRRPWAEQPWACLGL), and a premature stop (Fig. 1). The BLAST analysis of the 28 newly added residues (GRTPRSGPHSCWMSRRPWAEQPWACLGL) did not reveal significant similarity to any known protein.

### Protein Stability

As the initial step, we hypothesized that *HSF4* mutant proteins may be unstable. In order to evaluate the protein turnover rate, HEK293 cells were transiently transfected with clones encoding WT, G199EfsX15, R405X, and M419GfsX29 mutant proteins. Following transfection, cells were subjected to cycloheximide (CHX) treatment to inhibit protein synthesis and then whole cell lysates were analyzed by Western blotting. No statistically significant differences were observed between protein levels of WT, G199EfsX15, R405X, and M419GfsX29 evaluated up to 6 hours following the CHX treatment (not shown). Therefore, we concluded that protein stability did not play a role in the disease mechanism.

### Subcellular Localization

Previous studies have shown that the nucleus is the major pool for *HSF4b*, although the *HSF4b* protein had been identified in both the nucleus and cytosol.<sup>10</sup> However, to date the nuclear localization signal (NLS) for *HSF4* has not yet been identified. We set out to investigate if a loss of the C-terminal end in the G199EfsX15, R405X, and M419GfsX29 mutant *HSF4* proteins was associated with a loss of the NLS and consequently, abnormal trafficking to the nucleus. The *in silico* evaluation of the *HSF4b* protein (NP\_001035757), using the PredictProtein server (available in the public domain at [www.predictprotein.org](http://www.predictprotein.org))<sup>15</sup> did not identify any putative NLS sequences. Therefore, we proceeded to investigate experimentally if trafficking of the mutant *HSF4* proteins differed from the WT protein. FLAG-tagged WT and mutant *HSF4* clones were transiently transfected into HeLa cells. Immunocytochemical analysis with anti-FLAG antibody identified that WT *HSF4*, as well as G199EfsX15, R405X, and M419GfsX29 mutant *HSF4* proteins were localized primarily to the nuclei of transfected cells (Figure 2). This finding indicated that the trafficking of G199EfsX15, R405X, and M419GfsX29 mutant *HSF4* proteins to the nucleus was not compromised. In addition to being in the nucleus, WT and mutant *HSF4* proteins localized to the nuclear granules even though the

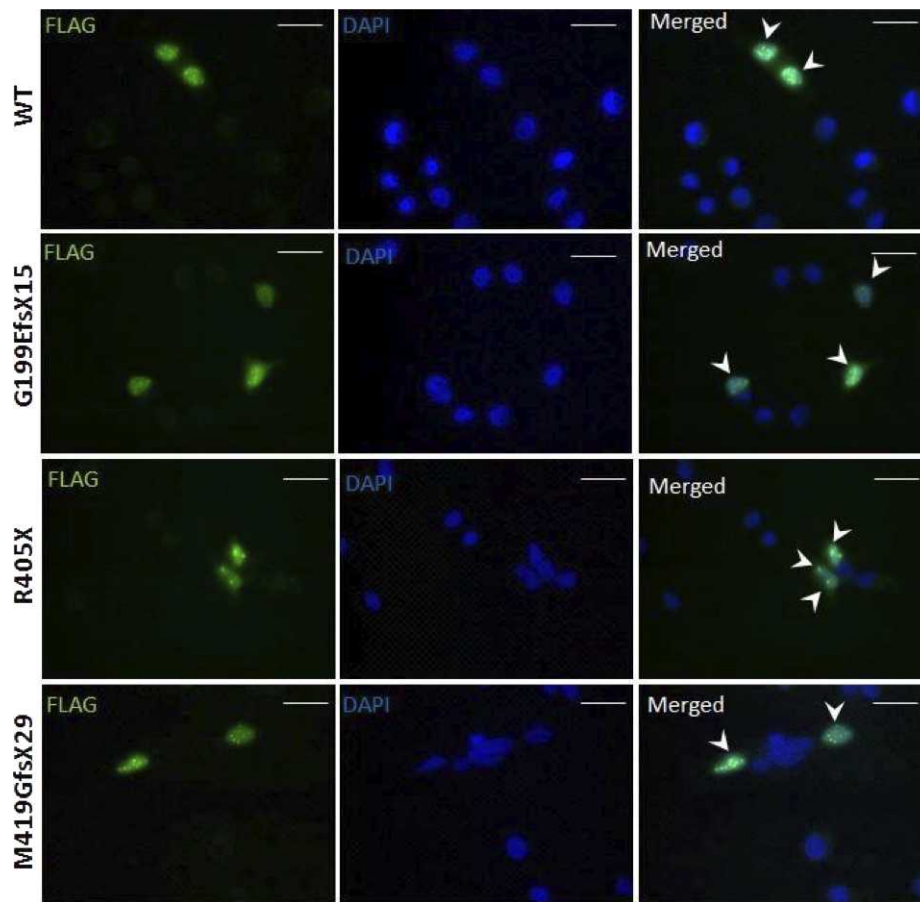


**FIGURE 2.** Subcellular localization of WT and mutant HSF4 proteins. WT, G199EfsX15, R405X, and M419GfsX29 FLAG-tagged HSF4 proteins were identified in transiently transfected HeLa nuclei following incubation with a FLAG antibody. Nuclei were counterstained with DAPI. Both WT and mutant HSF4 proteins were identified in nuclear granules (arrowheads). Scale bars: 25  $\mu$ m.

transfected cells were not subjected to any environmental stressors (Fig. 2).

### Western Blot and DNA-Binding Patterns

The *in silico* analysis with Compute pI/Mw tool (in the public domain at [http://web.expasy.org/compute\\_pi/](http://web.expasy.org/compute_pi/))<sup>16</sup> established that the predicted molecular weight for the FLAG-tagged WT HSF4b protein (NP\_001035757) is 54 kDa. The same analysis of the G199EfsX15, R405X, and M419GfsX29 mutant HSF4 proteins predicted molecular weights to be 25 kDa, 45 kDa, and 50 kDa, respectively. The Western blot analysis of nuclear (Fig. 3A) fractions from HEK293 cells transiently transfected with WT and mutant *HSF4* FLAG-tagged clones revealed FLAG immunoreactive bands that matched predicted molecular weights for the WT and mutant HSF4 proteins.

Next, we focused on the DNA-binding properties of WT and mutant HSF4 proteins. WT HSF4 protein formed a complex with the HSE containing oligonucleotide (Fig. 3B). Specificity of WT HSF4 binding to HSE was determined by a specific competition with unlabeled HSE, nonspecific competition with unlabeled SP1, and supershift with FLAG-antibody. The EMSA analysis of G199EfsX15 and M419GfsX29 mutant proteins also formed an HSE containing oligonucleotide complex, but with what appeared to be a weaker affinity when compared with WT. In contrast, the R405X mutant formed a complex with the HSE with an increased affinity compared with WT. The shifted bands of the G199EfsX15, R405X, and M419GfsX29 did not migrate as far as the shifted

bands in WT reflecting the lower molecular weight of these mutant HSF4 proteins when compared with WT. The specificity of observed shifted bands for G199EfsX15, R405X, and M419GfsX29 mutant proteins was confirmed by a specific competition with unlabeled HSE, nonspecific competition with unlabeled SP1, and supershift with anti-FLAG antibody (Fig. 3B).

### Transactivation of WT and Mutant HSF4 Proteins

Next, we focused on the transactivation potential of WT and mutant HSF4 proteins. It has been shown previously that HSF4 binds to the HSE elements of the  $\gamma$ C-crystallin and  $\alpha$ B-crystallin promoters.<sup>11-13,17-19</sup> Therefore, we evaluated the transactivation potential of WT and mutant HSF4 proteins using Luciferase reporters containing HSE elements from the human  $\gamma$ C-crystallin (pGL3.HSE-GC) and  $\alpha$ B-crystallin (pGL3.HSE-AB) promoters. The cotransfection of the *HSF4* clone encoding WT protein and the pGL3.HSE-GC and pGL3.HSE-AB reporter vectors caused an approximately 10-fold increase in activation when compared with the reporter vectors alone (Figs. 4A, 4B). The cotransfection of clones encoding G199EfsX15, R405X, and M419GfsX29 mutant proteins with pGL3.HSE-GC exhibited 4.87%, 9.41%, 45.82% of the activity of WT HSF4 and cotransfection with pGL3.HSE-AB exhibited 1.44%, 7.34%, and 8.32% of the activity of WT HSF4, respectively. These findings demonstrated significantly ( $P < 0.05$ ) reduced transactivation potential of all mutant HSF4 proteins when compared with WT HSF4.

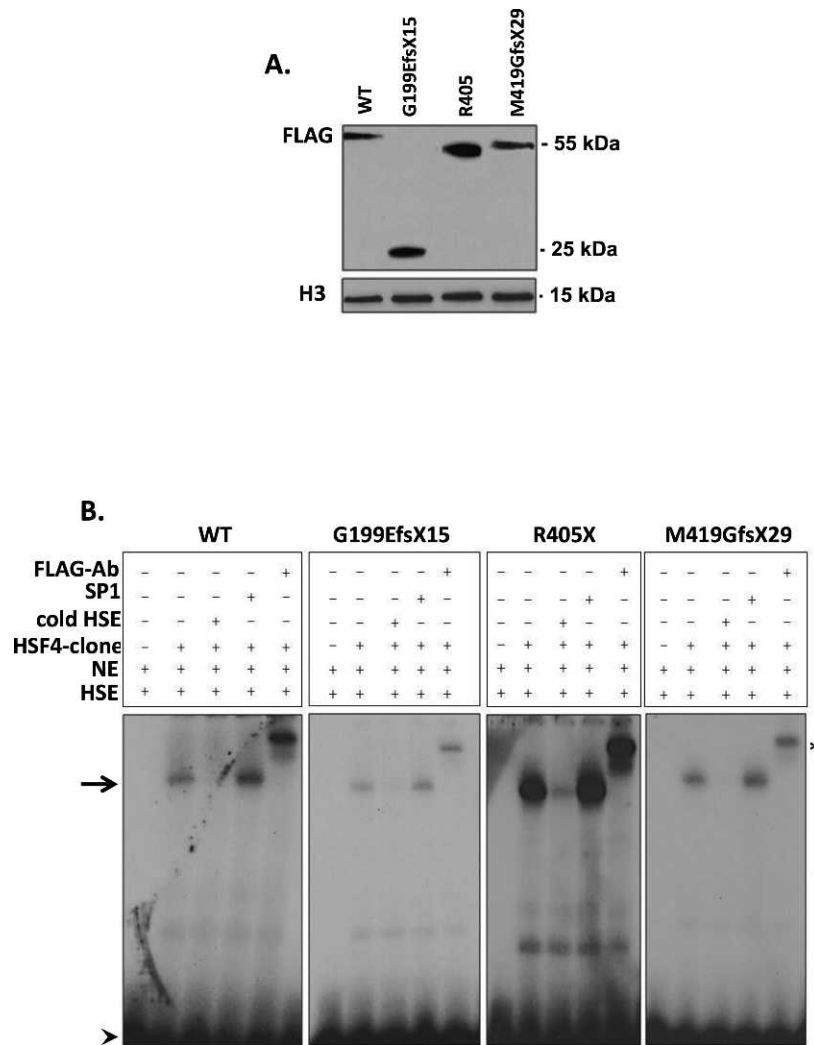


**FIGURE 3.** Western blot and EMSA of WT and mutant *HSF4* proteins. **(A)** Western blot analysis of nuclear extracts used in EMSA experiments shown in **(B)** from transiently transfected cells with WT and mutant *HSF4* FLAG-tagged clones following immunoblotting with a FLAG antibody and subsequently immunoblotted with an H3 antibody. **(B)** EMSA revealed that WT *HSF4* from nuclear extracts (NE) formed a complex with labeled HSE (*arrow*); the specificity of the *HSF4*-HSE complex was confirmed by specific competition with an unlabeled HSE oligo (cold HSE), by nonspecific competition with an unlabeled SP1 oligo (SP1) and supershift following addition of FLAG antibody (*asterisk*); *arrowhead* points to the unbound HSE containing primer. No DNA-protein complexes were observed with nuclear extracts from untransfected cells that did not contain an *HSF4*-clone. The G199EfsX15 and M419GfsX29 mutant proteins also formed a complex with the HSE, but with reduced affinity when compared with WT. The R405X mutant formed a complex with the HSE with a greater affinity than WT.

**The Analysis of the C-Terminal Region for Functional Domains**

It has been shown previously that the *HSF4b* C-terminal domain acts as an activator as opposed to the *HSF4a* that acts as a repressor.<sup>10</sup> To further evaluate the functional significance of the C-terminal end, we created a series of *HSF4* C-terminal deletion mutants (Fig. 5A). The mutant proteins were subjected to the same transcription activation assay containing the  $\gamma$ C-crystallin Luciferase reporter (Fig. 5B) and containing the  $\alpha$ B-crystallin Luciferase reporter (Fig. 5C) as before. The presence of the region containing the downstream of heptad repeat (DHR) region ( $\Delta$ 425-492) restored activation activity to the levels of the WT *HSF4* protein (Figs. 5B, 5C). However, the presence of an additional 10 amino acids ( $\Delta$ 435-492) failed to transactivate  $\gamma$ C-crystallin and  $\alpha$ B-crystallin Luciferase reporters showing only 5% for both reporters of the WT *HSF4* activation activity. Deletion mutants  $\Delta$ 445-492 and  $\Delta$ 455-492 exhibited increased activation activity to 37% and 68%, respectively, for the  $\gamma$ C-crystallin and

20% and 60%, respectively, for the  $\alpha$ B-crystallin Luciferase reporter. The  $\Delta$ 465-492 mutant protein exhibited activity that did not significantly differ from WT *HSF4* with both  $\gamma$ C-crystallin and  $\alpha$ B-crystallin Luciferase reporters.

We also wanted to determine if the region encompassing amino acid (aa) residues 245 to 319 specific for *HSF4b* was required for activation mediated by the region between aa residues 395 to 465. Our results showed that the  $\Delta$ 246-319 mutant *HSF4* protein exhibited an increase in activation activity with  $\gamma$ C-crystallin Luciferase reporter (213%) and  $\alpha$ B-crystallin Luciferase reporter (136%) when compared with the WT *HSF4* suggesting that this region suppresses transcriptional activation.

**DISCUSSION**

In this study, we demonstrate that three previously uncharacterized *HSF4* autosomal recessive mutations (c.595\_599delGGGCC, c.1213C>T, c.1327+4A>G)<sup>3-5</sup> are loss-of-function mutations. Our

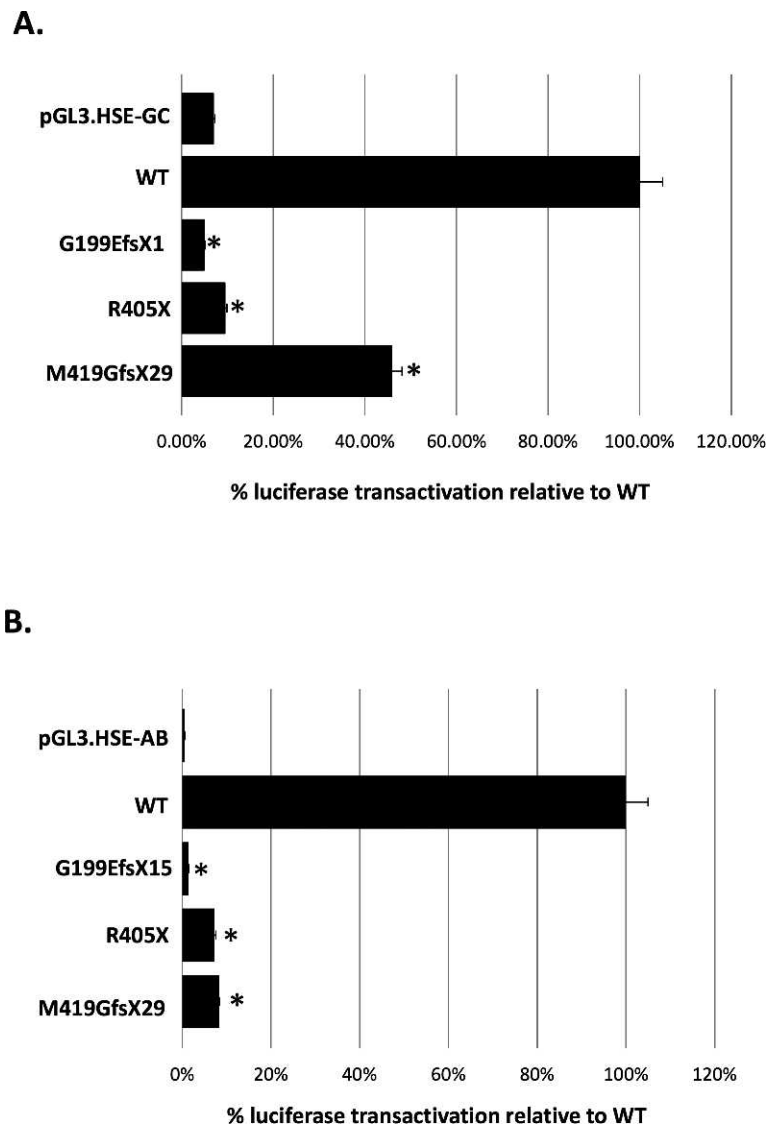


**FIGURE 4.** HSE-mediated transactivation of WT and mutant HSF4 proteins. Activation of the HSE-reporters containing promoter regions from  $\gamma$ C-crystallin (pGL.HSE-GC) (A) and  $\alpha$ B-crystallin (pGL.HSE-AB) (B) by WT and mutant HSF4 proteins. Luciferase values were normalized to  $\beta$ -galactosidase activity, averaged for three separate transfections and expressed relative to the ratio for WT HSF4. Error bars represent SEM. Asterisks indicate samples with a significant difference ( $P < 0.05$ ;  $t$ -test) calculated from comparison with WT.

results show that these three *HSF4* mutations encode truncated HSF4 mutant proteins that are stable and properly trafficked into the nucleus. Furthermore, our results showed that truncated HSF4 mutant proteins retain the ability to bind the HSE sequence in vitro. When compared to WT, G199EfsX15, and M419GfsX29 mutant proteins exhibited decreased HSE-mediated DNA binding affinity, whereas R405X mutant protein exhibited a greater affinity for HSE-mediated DNA binding. The molecular mechanism associated with the increase or decrease of HSE-mediated DNA binding affinity in these mutant HSF4 proteins is unclear. It is possible that novel amino acids added to the C-terminal ends of G199EfsX15 and M419GfsX29 mutant proteins decrease the trimer stability; conversely, a loss of 87 amino acids from the C-terminal end in R405X may increase the trimer stability. A decrease or an increase of the HSF4 trimer stability would consequently affect the HSE-mediated DNA binding affinity. Regardless of their HSE-mediated DNA binding affinity, mutant HSF4 proteins exhibited severely compromised HSE-mediated transactivation of  $\gamma$ C-crystallin and  $\alpha$ B-crystallin promoters, although transactivation of the  $\alpha$ B-

crystallin luciferase reporter seemed more severely affected. The differential effects of HSF4 mutations on the  $\gamma$ C-crystallin and  $\alpha$ B-crystallin promoters were reported previously<sup>12</sup> and were hypothesized to be due to differences in HSE structure: the  $\gamma$ C-crystallin promoter contains an atypical HSE structure consisting of multiple GAA-like sequences,<sup>14</sup> whereas the  $\alpha$ B-crystallin promoter contains a 3P-type HSE.<sup>14,18</sup>

Given that truncated HSF4 mutants retained the HSE-mediated DNA binding ability and lost the HSE-mediated transactivation ability provided the evidence that an activation domain or domains essential for HSF4 function may be present at the C-terminus. By using a series of plasmid constructs containing various portions of the HSF4 C-terminal end, we identified two segments essential for activation and two segments essential for suppression of the HSF4-mediated transcriptional activation (Fig. 6A). The first C-terminal activation domain is located within the DHR domain encompassing residues 395 to 424 (Fig. 6B), a region previously identified as a region of identity following comparison of HSF4

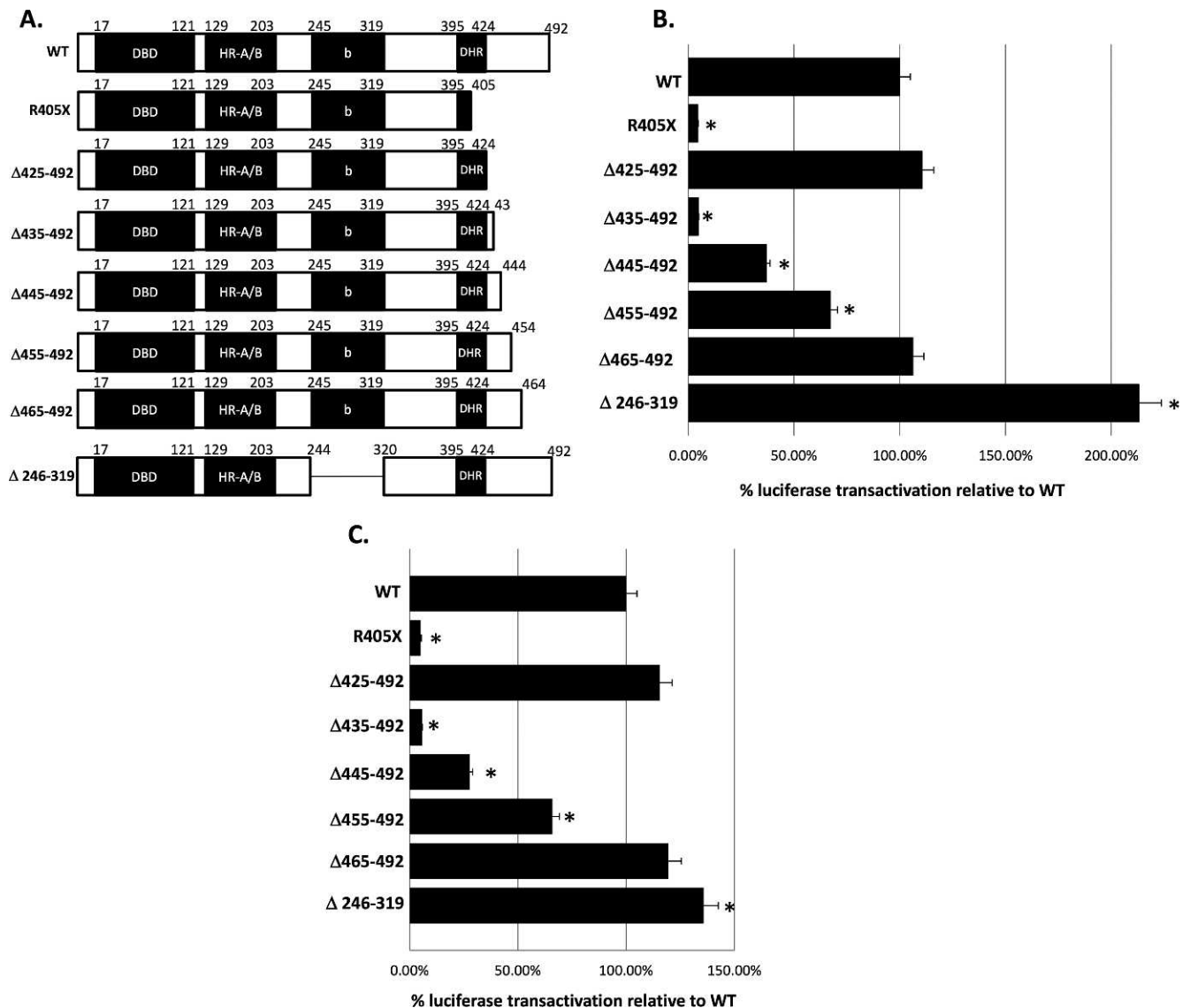


**FIGURE 5.** Deletion analysis of the C-terminal domain of HSF4b. The schematic representation of deletion constructs is shown in (A). Luciferase activity from the  $\gamma$ C-crystallin (pGL.HSE-GC) Luciferase reporter assay is shown in (B) and from the  $\alpha$ B-crystallin (pGL.HSE-AB) Luciferase reporter assay is shown in (C). Luciferase values were normalized to  $\beta$ -galactosidase activity, averaged for three separate transfections, and expressed relative to the ratio for WT HSF4. Error bars represent SEM. Asterisks indicate samples with a significant difference ( $P < 0.05$ ;  $t$ -test) calculated from comparison with WT.

with HSF1, HSF2, and HSF3.<sup>20</sup> An additional HSF4 activation domain resides between residues 435 to 464 that overlap with the syntenic regions of the second activation domain (AD2) in HSF1 (residues 431–505; Fig. 6B). Our results also show that the two HSF4 activation domains are separated by 10 amino acids (residues 425–434) exhibiting negative regulatory activity. In addition, the sequence domain unique to HSF4b (residues 245–319) also appears to exhibit negative regulation. These findings collectively indicate that the transcriptional activation in HSF4 is mediated by interactions between negative regulatory domains and transcription activator domains.

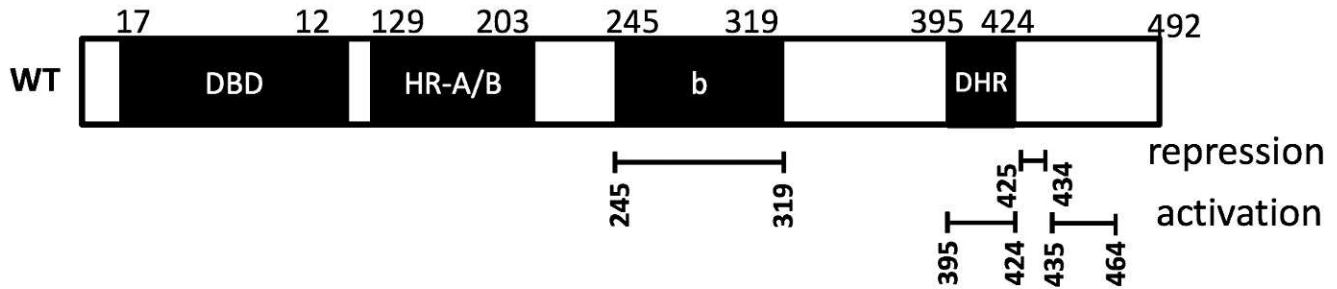
Previous studies have shown that HSF1 activation domains AD1 and AD2 are involved in both transcriptional initiation and elongation.<sup>21</sup> The AD1 domain contains a 17-amino acid region that interacts with the general transcriptional cofactor TAF9 (TAFII31).<sup>22</sup> Additionally, phenylalanine residues from both AD1 and AD2 domains associate with BRG1, an ATPase

subunit of the SWI/SNF chromatin remodeling complex.<sup>23</sup> It has been shown previously that HSF4 also recruits BRG1 to the promoter of target genes during the G1 phase of the cell cycle.<sup>24</sup> In mice, BRG1 is indispensable for mouse lens fiber cell differentiation and lens fiber cell denucleation.<sup>25</sup> Although HSF1 and HSF4 C-terminal domains lack amino acid sequence conservation, our studies suggest that the overall conservation of function may be preserved.

Further studies are needed to establish the precise amino acids within the HSF4 C-terminal region essential for recruitment of transcriptional initiation and elongation factors essential for HSF4 function.

In summary, our results show that three previously reported HSF4 mutations identified in families with autosomal recessive cataracts are loss of function mutations. These three mutations encode mutant HSF4 proteins with missing C-terminal domains. Detailed functional mapping of the C-terminal regions on HSF4b identified the presence of novel regulatory

**A.**



**B.**

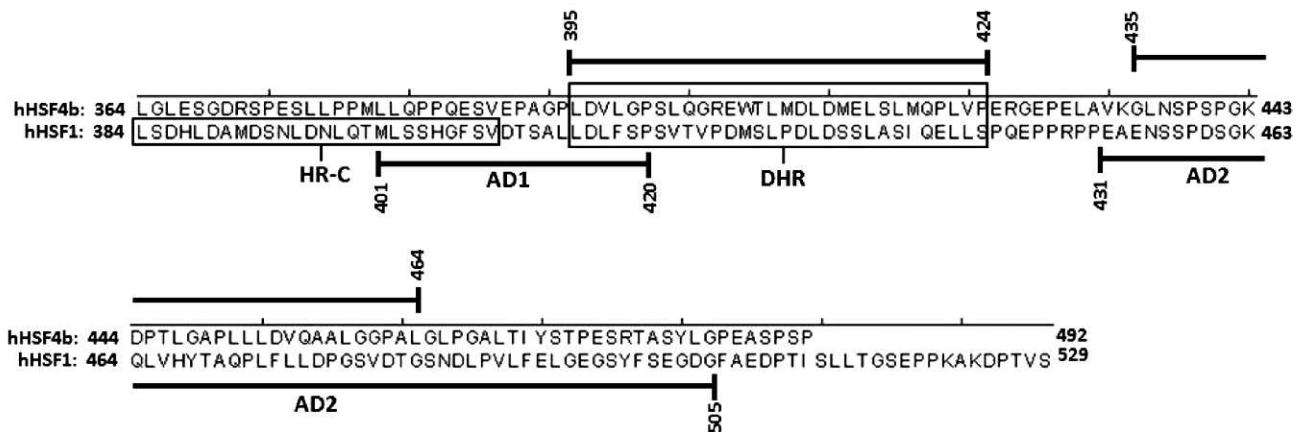


**FIGURE 6.** Localization of functional domains in human HSF4b. (A) Localization of the DBD, HR-A/B, sequence specific for HSF4b (b), and DHR domain were previously identified.<sup>10</sup> Two negative regulatory domains and two activation domains are depicted at the *bottom* with numbers referring to the amino acid residues in HSF4b (NP\_001035757). (B) Alignment of the C-terminal regions of human HSF4b (*top*) and HSF1 (*bottom*). The HR-C domain is only present in HSF1, whereas the DHR domain is present in both HSF4b and HSF1. The HSF1 activation domain 1 (AD1) and activation domain 2 (AD2) are depicted on the *bottom*; on *top* are activation domains identified in HSF4b. The *numbers* refer to the amino acid residues for the HSF4b protein (NP\_001035757) and HSF1 (NP\_005517).

domains essential for normal HSF4 function. Given that all three mutant HSF4 proteins lack these regulatory domains, our findings indicate that the loss of HSF4 function is due to a loss of C-terminal regulatory domains.

**Acknowledgments**

The authors thank Elena Semina, PhD (Medical College of Wisconsin), for helpful discussions. We also thank Brad Endres (Medical College of Wisconsin) and Michael A. Maier (Maier Learning Media) for their technical assistance.

Supported by the National Eye Institute/National Institutes of Health Grant EY18872 (DJS) and a National Research Service Award Training Grant T32-EY014537 (KM) from the National Institutes of Health.

Disclosure: **K. Merath**, None; **A. Ronchetti**, None; **D.J. Sidjanin**, None

**References**

1. Bu L, Jin Y, Shi Y, et al. Mutant DNA-binding domain of HSF4 is associated with autosomal dominant lamellar and Marner cataract. *Nat Genet.* 2002;31:276-278.
2. Ke T, Wang QK, Ji B, et al. Novel HSF4 mutation causes congenital total white cataract in a Chinese family. *Am J Ophthalmol.* 2006;142:298-303.
3. Forshew T, Johnson CA, Khaliq S, et al. Locus heterogeneity in autosomal recessive congenital cataracts: linkage to 9q and germline HSF4 mutations. *Hum Genet.* 2005;117:452-459.
4. Sajjad N, Goebel I, Kakar N, Cheema AM, Kubisch C, Ahmad J. A novel HSF4 gene mutation (p.R405X) causing autosomal recessive congenital cataracts in a large consanguineous family from Pakistan. *BMC Med Genet.* 2008;9:99.
5. Smaoui N, Beltaief O, BenHamed S, et al. A homozygous splice mutation in the HSF4 gene is associated with an autosomal recessive congenital cataract. *Invest Ophthalmol Vis Sci.* 2004; 45:2716-2721.

6. Wu C. Heat shock transcription factors: structure and regulation. *Annu Rev Cell Dev Biol.* 1995;11:441-469.
7. Akerfelt M, Morimoto RI, Sistonen L. Heat shock factors: integrators of cell stress, development and lifespan. *Nat Rev Mol Cell Biol.* 2010;11:545-555.
8. Sorger PK, Nelson HC. Trimerization of a yeast transcriptional activator via a coiled-coil motif. *Cell.* 1989;59:807-813.
9. Pirkkala L, Nykanen P, Sistonen L. Roles of the heat shock transcription factors in regulation of the heat shock response and beyond. *FASEB J.* 2001;15:1118-1131.
10. Tanabe M, Sasai N, Nagata K, et al. The mammalian HSF4 gene generates both an activator and a repressor of heat shock genes by alternative splicing. *J Biol Chem.* 1999;274:27845-27856.
11. Fujimoto M, Izu H, Seki K, et al. HSF4 is required for normal cell growth and differentiation during mouse lens development. *EMBO J.* 2004;23:4297-4306.
12. Enoki Y, Mukoda Y, Furutani C, Sakurai H. DNA-binding and transcriptional activities of human HSF4 containing mutations that associate with congenital and age-related cataracts. *Biochim Biophys Acta.* 2010;1802:749-753.
13. Liang L, Liegel R, Endres B, Ronchetti A, Chang B, Sidjanin DJ. Functional analysis of the Hsf4(lop11) allele responsible for cataracts in lop11 mice. *Mol Vis.* 2011;17:3062-3071.
14. Yamamoto N, Takemori Y, Sakurai M, Sugiyama K, Sakurai H. Differential recognition of heat shock elements by members of the heat shock transcription factor family. *FEBS J.* 2009;276:1962-1974.
15. Rost B, Yachdav G, Liu J. The PredictProtein server. *Nucleic Acids Res.* 2004;32:W321-W326.
16. Gasteiger E, Gattiker A, Hoogland C, Ivanyi I, Appel RD, Bairoch A. ExPASy: The proteomics server for in-depth protein knowledge and analysis. *Nucleic Acids Res.* 2003;31:3784-3788.
17. Shi X, Cui B, Wang Z, et al. Removal of Hsf4 leads to cataract development in mice through down-regulation of gamma S-crystallin and Bfsp expression. *BMC Mol Biol.* 2009;10:10.
18. Somasundaram T, Bhat SP. Developmentally dictated expression of heat shock factors: exclusive expression of HSF4 in the postnatal lens and its specific interaction with alphaB-crystallin heat shock promoter. *J Biol Chem.* 2004;279:44497-44503.
19. Min JN, Zhang Y, Moskophidis D, Mivechi NE. Unique contribution of heat shock transcription factor 4 in ocular lens development and fiber cell differentiation. *Genesis.* 2004;40:205-217.
20. Nakai A, Tanabe M, Kawazoe Y, Inazawa J, Morimoto RI, Nagata K. HSF4, a new member of the human heat shock factor family which lacks properties of a transcriptional activator. *Mol Cell Biol.* 1997;17:469-481.
21. Brown SA, Weirich CS, Newton EM, Kingston RE. Transcriptional activation domains stimulate initiation and elongation at different times and via different residues. *EMBO J.* 1998;17:3146-3154.
22. Piskacek S, Gregor M, Nemethova M, Grabner M, Kovarik P, Piskacek M. Nine-amino-acid transactivation domain: establishment and prediction utilities. *Genomics.* 2007;89:756-768.
23. Sullivan EK, Weirich CS, Guyon JR, Sif S, Kingston RE. Transcriptional activation domains of human heat shock factor 1 recruit human SWI/SNF. *Mol Cell Biol.* 2001;21:5826-5837.
24. Tu N, Hu Y, Mivechi NE. Heat shock transcription factor (Hsf)-4b recruits Brg1 during the G1 phase of the cell cycle and regulates the expression of heat shock proteins. *J Cell Biochem.* 2006;98:1528-1542.
25. He S, Pirity MK, Wang WL, et al. Chromatin remodeling enzyme Brg1 is required for mouse lens fiber cell terminal differentiation and its denucleation. *Epigenetics Chromatin.* 2010;3:21.